Localization of oxygen donor states in gallium nitride from first-principles calculations

K. C. Mishra
Central Research, OSRAM SYLVANIA, Beverly, Massachusetts 01915, USA

P. C. Schmidt and Stefan Laubach
Eduard-Zintl-Institut, Technische Universität Darmstadt, Petersenstrasse 20, D-64287 Darmstadt, Germany

K. H. Johnson
Department of Materials Science, Massachusetts Institute of Technology, Cambridge, Massachusetts 02139, USA
(Received 31 January 2007; revised manuscript received 16 April 2007; published 31 July 2007)

Using first-principles band structure methods, the electronic structure and local geometry of oxygen impurities in GaN have been investigated as a function of oxygen concentration. The concentrational variation has been simulated using various supercells. In order to test the validity of "rigid band" models usually employed to describe the effect of impurities on the electronic structure and associated properties of wide band gap semiconductors, the spatial localization of donor states associated with oxygen atoms at the nitrogen site has been carefully explored. For all the supercells studied in this work, the energy bands near the bottom of the conduction band are found to be severely perturbed. The donor electrons are found to occupy extended states. However, with increasing dilution of impurities, the donor electron tends to localize near the impurity ion. This localization monotonically progresses with decreasing oxygen concentration.

DOI: 10.1103/PhysRevB.76.035127 PACS number(s): 71.20.−b

I. INTRODUCTION

Thin films of gallium nitride (GaN) and its alloys with nitrides of aluminum and indium are being extensively investigated for their application in light emitting diodes. Nitride based lighting devices are expected to be more efficacious and to be also a mercury-free light source alternative of the future to fluorescent lamps based on Hg-discharge technology.[1] However, there remain many questions regarding the optical and electrical properties of III-V nitrides, which need to be thoroughly understood for maximizing the electrical-to-visible energy conversion process within light emitting diodes. One important topic is the dependence of structural, optical, and electrical properties of GaN on the lattice defects and impurities. In this paper, the effects of oxygen impurities in GaN on its electronic structure and associated properties are investigated using first-principles band structure methods.

Unintentional contamination of GaN with ambient oxygen during synthesis continues to be a problem in the synthesis of GaN powders[2,3] and thin films.[4] Oxygen atoms are easily incorporated into GaN because of the relative stability of Ga-O bonds compared to the Ga-N bonds. The enthalpy of formation of Ga-O bonds is −545 kJ/mol, which is significantly higher than −110 kJ/mol for GaN bonds.[5] The GaN lattice can accommodate nearly 25 at. % of oxygen without any change in its wurtzite crystal structure or precipitation of a second phase.[6] At higher oxygen concentration, the coordination of gallium atoms most likely changes from tetrahedral to octahedral, resulting in an overall amorphous structure.[3] The change in coordination is most likely due to the fact that the octahedral coordination of Ga with O is thermodynamically more stable. Gallium oxide, Ga_2O_3, crystallizes into two crystalline phases, α and β, with octahedrally coordinated Ga atoms being present in both but tetrahedrally coordinated Ga only in the β phase.[7,8] No stable oxides of Ga with nitrogen impurities substituting for oxygen have been reported.[9]

Extended x-ray absorption fine structure (EXAFS) measurements probing the local coordination of Ga have shown that the local tetrahedral coordination of Ga atoms is preserved even with a high concentration of oxygen impurity.[10] For thin films prepared by the ion assisted deposition method, the total electron yield x-ray absorption spectroscopy measurements of the local structure showed that the average Ga-ligand bond length decreased from 1.938 Å in the wurtzite structure. At a low concentration of oxygen resulting from a longer deposition time, the average bond lengths in the first coordination sphere are found to be comparable or slightly higher than the normal Ga-N bond length.[10]

In addition to any structural modification, the oxygen atoms substituting for the nitrogen atoms in III-V semiconductors lead to *n*-type conductivity.[11] An oxygen atom substituting for a nitrogen atom, designated as O_N^X in the Kroger-Vink notation[12] creates a donor level in the band gap. This donor level would have the characteristics of an antibonding sp^3-hybridized state of Ga and O since all the bonding states are fully occupied and belong to occupied states in the valence band. In this sense, this impurity induced donor level due to an oxygen atom substituting for a nitrogen atom can be viewed as a perturbed state at the bottom of the conduction band. Due to the positively charged point defect $O_N^{\bullet}$ instead of N_N^X, the corresponding energy level is lowered into the band gap. This donor level associated with $O_N^{\bullet}$ holding the electron released from the substitution process ultimately frees the electron with increasing temperature and contributes to the *n*-type behavior of GaN.

At lower concentrations of oxygen impurities at the ppm level, GaN maintains charge neutrality by accommodating the excess electrons in the conduction band states, as dis-

cussed earlier. However, at higher concentrations of oxygen, oxygen impurities substituting for the nitrogen atoms could intrinsically lead to Ga vacancies or similar point defects for compensating the charge deficiency arising from the substitution process.[12] Extrinsically, the charge compensation could also be maintained by replacing trivalent gallium atoms with divalent ions such as zinc. The case of Zn_{Ga} has been investigated in this work in order to appreciate how vacant donor states affect the overall electronic structure of GaN with oxygen impurities.

Calculations reported in this work are performed using supercell band structure methods. We have investigated modifications of local geometries in the vicinity of $O_N^{\bullet}$ and the electronic structures of GaN as a function of oxygen concentration. In the "rigid band" models of semiconductors, the donor levels are normally viewed as localized states. Optical and electrical properties of doped semiconductors are normally analyzed using these rigid band models. It will be shown that such models are only valid for $O_N^{\bullet}$ centers in the limit of extreme dilution, perhaps at a donor concentration of $10^{-18}-10^{-20}/\mathrm{cm}^{-3}$, which corresponds to a typical dopant concentration in intentionally doped samples for device application. Since these donor levels originate from the perturbed conduction band states and are very close in energy to the bottom of the conduction band, these donor states should form extended states even at moderate concentrations. This has indeed been observed in the present work and are relevant in understanding optical properties of GaN with high oxygen concentration, as in most powder samples.

II. THEORY

The Vienna *ab initio* simulation package (VASP)[13] and augmented spherical wave (ASW)[14] approach were used in this work for calculating the band structures of GaN and $GaN_{1-x}:O_x$ for values of x varying from 0 to 0.5. The local structural relaxations due to the incorporation of oxygen atoms at the nitrogen sites were first simulated using VASP. VASP implements a quantum mechanical molecular dynamic simulation algorithm, from which we have chosen the projector augmented plane wave basis functions[15,16] and a generalized gradient correction approximation (GGA) for the exchange-correlation potential.[17]

The optimized structural data from VASP were then used as structural input for calculating the electronic structures of GaN with and without oxygen impurities using the ASW method with a scalar-relativistic correction. The band structures calculated by both VASP and ASW programs are almost identical for the systems considered here. However, the electronic structure calculated by the ASW method lends itself to a simpler interpretation of the chemical bonding in terms of the valence electrons; therefore the bonding structure in the neighborhood of O will be discussed using results from this approach.

The ASW method uses the atomic sphere approximation with atomic spheres and empty spheres occupying interstitial positions. A sphere geometry optimization algorithm was employed for an optimal choice of empty sphere positions and their radii.[18]

The requirement of a minimal basis set in this approach makes it relatively faster compared to VASP in calculating the band structure of a material on a larger k mesh in the Brillouin zone. In the present case, the basis sets include $O(2s,2p)$, $N(2s,2p)$, and $Ga(4s,4p,3d)$. The Barth-Hedin exchange-correlation potential and a $12\times12\times12$ k mesh in the full Brillouin zone were applied.[19] Calculations with finer k meshes and different exchange-correlation potentials show this choice to be adequate.

The main objective of this theoretical investigation is to study relaxation in the local geometry and the perturbation of the electronic structure of GaN with increasing oxygen concentration with and without any explicit charge compensating mechanism. Supercells with dimensions $1\times1\times1$ (regular cell), $2\times2\times2$, $3\times3\times2$, and $4\times4\times3$ and having only one oxygen atom per cell were used to study the effect of oxygen concentration on the band structure of GaN. This choice of supercells corresponds to a variation of oxygen concentration of 25–0.5 at. %. The lower limit is still a high level of oxygen impurities compared to impurity concentration in an intentionally doped material, yet not unreasonable for powder samples.

Calculations for GaN:O were performed in two different ways. In the first case, a scheme without any explicit charge compensation was adopted, and therefore every supercell, when electrically neutral, represents a n-type material with excess electrons occupying modified conduction band states. How the conduction band states are modified to accommodate these electrons will be investigated. In the second case, a substitutional zinc atom at a gallium site is used per oxygen atom for charge compensation. This is essentially a charge compensating procedure and is often adopted in the synthesis of ionic solids to maintain the correct charge state of the dopants. Since the ionic radii of Zn and Ga are comparable, Zn atoms are chosen as the charge compensating ions substituting for the Ga atoms. Such a substitutional scheme generates no free electrons after the valence band states are fully occupied. Thus, GaN should remain a large band gap semiconductor after this substitutional modification.

III. RESULTS

A. Variation in local geometry with oxygen impurity

In gallium nitride, both the Ga and N atoms occupy Wyckoff site $2b$ with site symmetry $3m$. Both the atoms are tetrahedrally coordinated to four nearest neighbors. Three of the four bond lengths are 1.941 Å and one is 1.977 Å.[20] This departure from an ideal T_d to C_{3V} site symmetry is easily explained in terms of the sp^3 hybridization of gallium and nitrogen atoms. The optimized structure for GaN using VASP (Table I) is in good agreement with experiment.[20]

The optimized structures of GaN:O for a regular unit cell, Ga_2NO, a $2\times2\times2$ supercell, $Ga_{16}N_{15}O$, and a $3\times3\times2$ supercell, $Ga_{36}N_{35}O$, are listed in Table I. The last two columns list a range of the Ga-N and O-Ga bond lengths describing the coordination of Ga and O atoms. The oxygen atoms substituting for nitrogen atoms remain tetrahedrally coordinated. The O-Ga bond lengths vary from 2.02 to 2.08 Å, and those for N-Ga from 1.93 to 2.07 Å. The EXAFS[10] measurements

TABLE I. Optimized structure for GaN:O.

Row	Supercell	a (Å)	c (Å)	$d_{\text{N-Ga}}$ (Å)	$d_{\text{O-Ga}}$ (Å)
1	GaN_{expt}	3.1891	5.1853	1.942–1.977	
2	Ga_2N_2	3.216	5.234	1.965–1.973	
3	Ga_2NO	3.271	5.531	1.978–2.068	2.017–2.075
4	$Ga_{16}N_{15}O$	3.231×2	5.266×2	1.954–1.987[a]	2.035–2.045
5	$Ga_{36}N_{35}O$	3.224×3	5.243×2	1.952–1.981	2.048–2.055
6	GaZnNO	3.233	5.290	1.947	1.946
7	$Ga_{15}ZnN_{15}O$	3.223×2	5.243×2	1.931–2.016[a]	2.042–2.068
8	$Ga_{35}ZnN_{35}O$	3.220×3	5.236×2	1.956–1.982	2.052–2.071

[a]Nearest neighbors are four-Ga, next nearest neighbors N or O.

showed that the average Ga and ligand bond lengths within the first coordination shell decrease compared to the Ga-N bond length in undoped GaN with increasing oxygen concentration. This discrepancy with experiment could be due to the microstructure of thin films and the partially unsaturated coordination although a fourfold coordination was assumed for data fitting.

In this context, it is useful to review the coordinations of Ga and O in gallium oxide, Ga_2O_3. In the α form, all of the Ga ions are coordinated to six oxygen atoms, and the oxygen atoms to four gallium atoms.[7] There are two sets of bond lengths: 1.921 and 2.077 Å. The latter is larger than the Ga-N bond length and the former is comparable. In the β form, there are two types of Ga ions, one tetrahedrally coordinated and the other octahedrally coordinated.[8] The oxygen atoms, in contrast, are coordinated to three or four Ga atoms. For tetrahedral coordination, the Ga-O bond lengths (1.803–1.853 Å) are shorter than the Ga-N bond lengths. But the bond lengths for the tetrahedrally coordinated oxygen atoms (1.853–2.077 Å) are larger than the Ga-N bond lengths. The latter values are in good agreement with the theoretically calculated O-Ga bond lengths.

One could argue that the structural optimization results in longer metal-ligand bond lengths because the charge neutrality is accomplished by accommodating electrons in the conduction band states. There is one excess electron per supercell, which reduces the effective charge on the cations, thus leading to longer bond lengths. In order to test if this is indeed the case, calculations were performed with one Zn atom per supercell occupying a Ga site in addition to an O atom occupying a N site. The charge compensating atom pairs of Zn and O were deliberately placed far apart from each other, namely, 6.725 and 4.627 Å in the supercells of $Ga_{16}N_{15}O$ and $Ga_{36}N_{35}O$ compared to the nearest N-Ga distance of 1.899 and 1.923 Å, respectively. The optimized metal-ligand bond lengths and the lattice vectors are also listed in Table I. In these cases, the point defects Zn_{Ga} and O_N lead to charge neutral pairs, and thus there are no free electrons. Thus, if there is any dependence of the metal-ligand bond lengths on the mechanism of maintaining charge neutrality, the optimized structural data for these supercells will reveal these effects. However, the structural parameters for these supercells show the same trend as those without any charge compensating scheme. The bond lengths calculated by these two different approaches differed by less than ~0.02 Å.

B. Variation of electronic structure of GaN:O with oxygen concentration

The band structures for various supercells studied in this work are shown in Figs. 1 and 2 along the symmetry direction, Γ-*A*-*L*-*H* of the Brillouin zone of a hexagonal lattice. The shapes of the bands along this direction as well as Γ-*M*-*K* (not shown in these figures) for pure GaN are in good agreement with those calculated by a linearized augmented plane wave method.[21] The ordering of the electronic states can be seen in Fig. 3, where we have plotted the partial density of states (DOS) for the $2\times2\times2$ supercell calculation. The highest occupied valence bands have a significant admixture of N 2*p*-, O 2*p*-, and Ga 4*p*-like states (Fig. 3). The occupied bands with a predominant O 2*p*-like character are located at lower energies compared to those with N 2*p*-like states. The states near the bottom of the conduction band are composed of 2*s*- and 2*p*-like states of O and N and 4*s*- and 4*p*-like states of Ga. The calculated optical band gap is 1.86 eV, which is about half the experimental value of 3.4 eV.[22] This discrepancy is associated with the density functional approximation and is extensively discussed in the literature.[23]

In Fig. 1, the band structure of GaN is compared with those of Ga_2NO and GaZnNO for the unit cell, $1\times1\times1$. In Ga_2NO, 50% of N has been substituted by O. Such high levels of oxygen concentration have been experimentally observed, as discussed earlier. GaZnNO is used as a model compound to study the effect of electrons in the conduction band on the electronic structure of the heavily doped system. In comparing the electronic structures of Ga_2NO and GaN, it is quite obvious that the degeneracy of the lowest energy conduction bands is removed along *A*-*L*-*H* directions. The lowest band bends down toward the valence band. This splitting is severe for GaZnNO compared to Ga_2NO. Both the systems have become essentially "metallic" with no energy gap. While the low lying conduction bands show a significant dispersion from Γ to *A*, two high lying valence bands show no dispersion along this direction. These states corre-

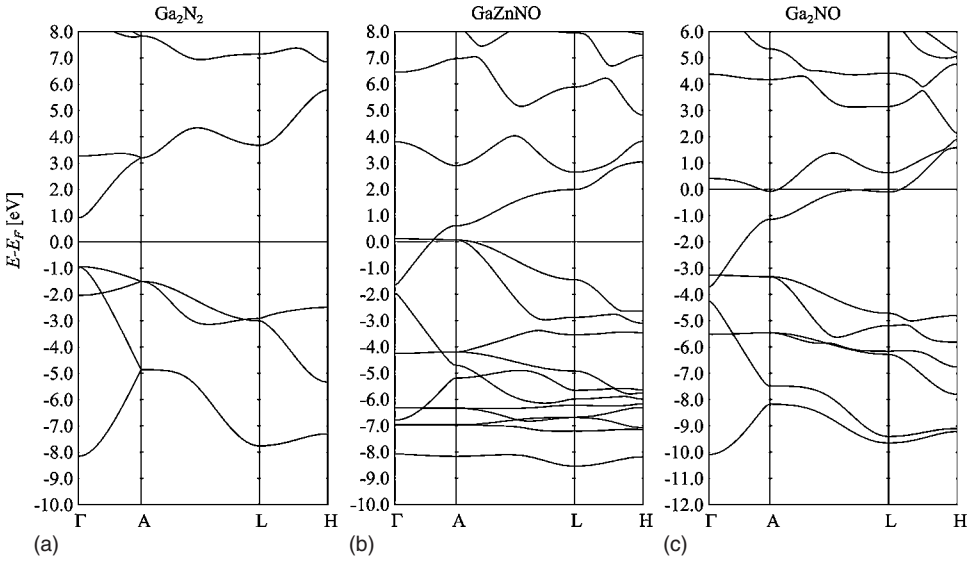

FIG. 1. Electronic band structure of the highest valence bands and the lowest conduction bands for Ga_2N_2, GaZnNO, and Ga_2NO hexagonal unit cells for the symmetry direction, Γ-*A*-*L*-*H* of the Brillouin zone. For the semiconductors, E_F is chosen as the middle between the maximum of the valence band and the minimum of the conduction band (a). For the metallic compounds, E_F is chosen as the top of the occupied donor states [(b) and (c)]. The Fermi energy E_F is the zero of the energy scale.

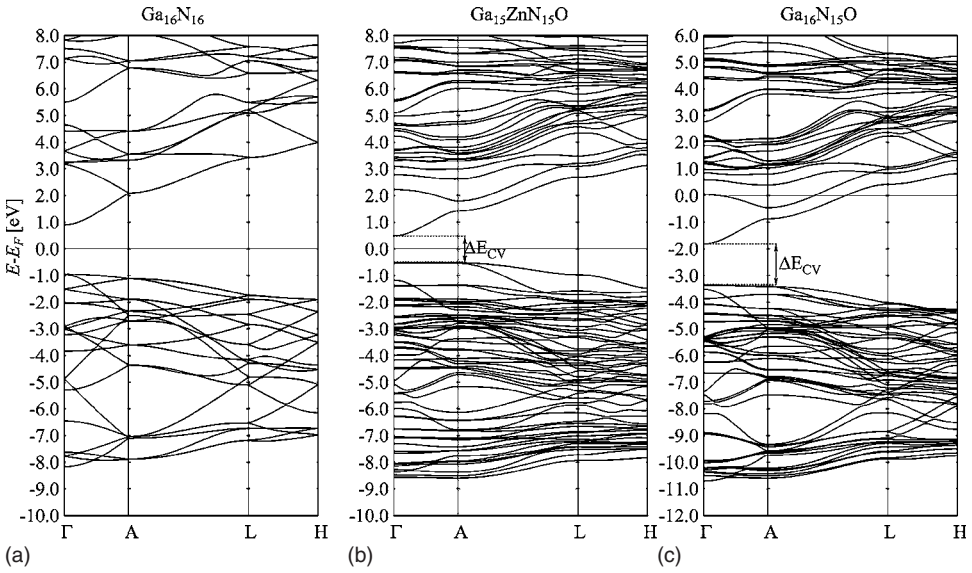

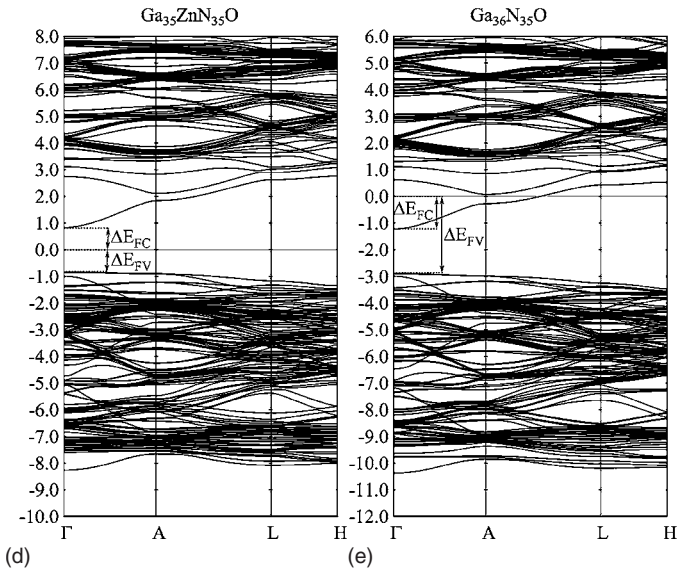

FIG. 2. Electronic band structure of the highest valence bands and the lowest conduction bands for $Ga_{16}N_{16}$, $Ga_{15}ZnN_{15}O$, $Ga_{16}N_{15}O$, $Ga_{35}ZnN_{35}O$, and $Ga_{36}N_{35}O$ hexagonal unit cells for the symmetry direction, Γ-*A*-*L*-*H* of the Brillouin zone. For the semiconductors, E_F is chosen as the middle between the maximum of the valence band and the minimum of the conduction band [(a), (b), and (d)]. For the metallic compounds, E_F is chosen as the top of the occupied donor states [(c) and (e)]. The Fermi energy E_F is the zero of the energy scale.

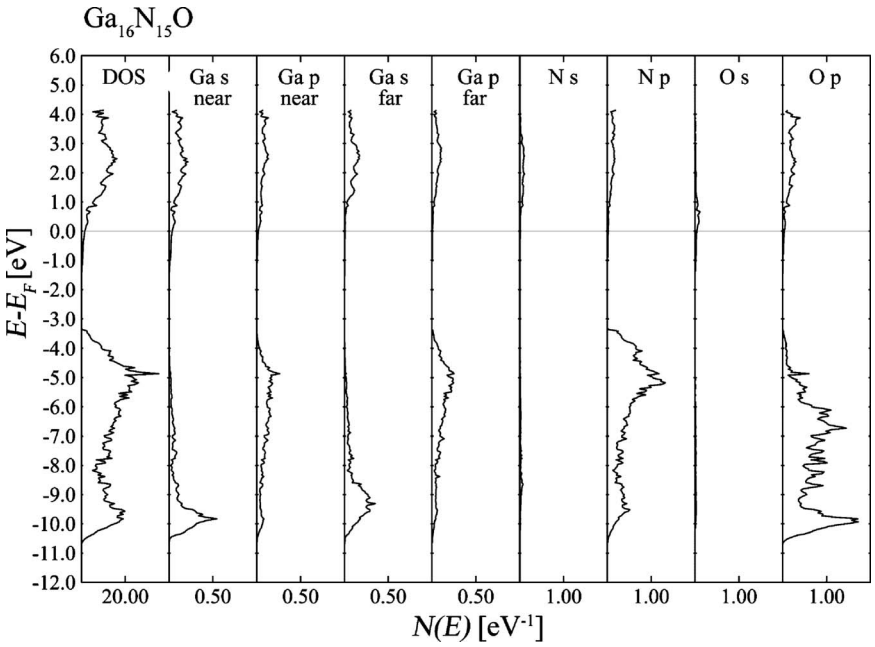

FIG. 3. Density of states (DOS) and partial DOS of the highest valence bands and the lowest conduction bands for $Ga_{16}N_{15}O$. For this metallic compound, E_F is chosen as the top of the occupied donor states. The Fermi energy E_F is the zero of the energy scale.

spond to electrons in nonbonding p-like states of N. In contrast to these localized states, the corresponding conduction band states are antibonding in nature with respect to nearest neighbors and bonding with respect to the second nearest neighbors and exhibit a significant dispersion characteristic of truly extended states.

The band structures for supercells $2\times2\times2$ and $3\times3\times2$ shown in Fig. 2 demonstrate the effect of dilution of oxygen impurity on the band structures. We have focused on the bands near the top of the valence band and the bottom of the conduction bands. Changes in these regions are critical for the electrical and optical properties of a material. For a better comparison with the undoped GaN, the band structure of pure GaN for a larger unit cell $(2\times2\times2)$ (smaller Brillouin zone) is also included in Fig. 2. Comparing GaN and GaN:O, one sees that no new band appears in the forbidden gap without any dispersion even for the largest supercell, which could indicate the presence of a localized donor level in the conventional sense. Therefore, we defined the top of the valence band, E_{VBM} as the maximum of the bands originating from Ga- and N-bonding states, and the bottom of the conduction band, E_{CBM}, as the minimum of the next band. The difference in energy between the two bands near the Γ point is chosen to be the band gap, $\Delta E_{\mathrm{CV}}=E_{\mathrm{CBM}}-E_{\mathrm{VBM}}$. It shall be pointed out that this band gap is not the optical band gap for those systems with occupied donor states. Figures 1 and 2 demonstrate that ΔE_{CV} decreases with increasing oxygen concentration. This gap completely disappears for GaN_2O corresponding to a 25 at. % concentration of oxygen. This is also true for $Ga_{1-x}Zn_xN_{1-x}O_x$. Thus, this lowering of the gap is not related to the occupancy of conduction-band-like states. The lowest conduction band states for Ga_2NO and GaZnNO have a similar dispersion in the k space. This similarity is more apparent for lower oxygen concentrations.

In addition to E_{CV}, the energy separation between the Fermi energy E_F and E_{CBM}, $(\Delta E_{\mathrm{FC}}=E_F-E_{\mathrm{CBM}})$ and also between E_F and E_{VBM} $(\Delta E_{\mathrm{FV}}=E_F-E_{\mathrm{VBM}})$ are listed in Table II. The values of ΔE_{FC} increases with increasing O concentration since more conduction band states need to be occupied to accommodate electrons freed by the substitution process. However, the quantity ΔE_{FV} indicates a maximum. The nonmonotonic behavior of ΔE_{FV} is a result of the different rates of change in the values of ΔE_{CV} and ΔE_{FC} with increasing oxygen concentration.

The shape of the energy bands near the Γ point suggests that electrons associated with O_N^X defects reside in delocalized states in the supercells. The band structure alone does not provide a complete description of the chemical bonding in GaN and of how the substitutional oxygen impurities modify this bonding structure. For this reason, the partial densities of states (PDOSs) for various supercells for the

TABLE II. Energy differences (in eV) for GaN:O. $\Delta E_{\mathrm{CV}}=E_{\mathrm{CBM}}-E_{\mathrm{VBM}}$ is the energy between the conduction band minimum E_{CBM} and the valence band maximum E_{VBM}; $\Delta E_{\mathrm{FC}}=E_F-E_{\mathrm{CBM}}$ is the difference between the Fermi level E_F and E_{CBM} and $\Delta E_{\mathrm{FV}}=E_F-E_{\mathrm{VBM}}$ is the difference between the Fermi level E_F and E_{VBM} (half the band gap for semiconductors). For the semiconductors, E_F is chosen as the middle between the maximum of the valence band and the minimum of the conduction band. For the metallic compounds, E_F is chosen as the top of the occupied donor states.

Supercell	ΔE_{CV}	ΔE_{FC}	ΔE_{FV}
$(GaN)_{\mathrm{expt}}$	3.38		
Ga_2N_2	1.86	−0.93	0.93
Ga_2NO	0	3.26	3.26
$Ga_{16}N_{15}O$	1.54	1.81	3.35
$Ga_{36}N_{35}O$	1.67	1.23	2.90
GaZnNO	0.0	0.0	0.0
$Ga_{15}ZnN_{15}O$	1.00	−0.50	0.50
$Ga_{35}ZnN_{35}O$	1.67	−0.89	0.89

donor states are plotted in Figs. 4(a)–4(c). The figures show the PDOS of O, one of the nearest gallium atoms Ga, and a pair of Ga and N atoms far removed. The data in Figs. 4(a)–4(c) are computed for the last occupied band(s) occupied by the electrons supposedly originating from O_N^X. Additionally, the electron density distributions for the lowest conduction (donor) state in the vicinity of the oxygen impurity are plotted in Fig. 5 for the $2\times2\times2$, $3\times3\times2$, and $4\times4\times3$ supercells. For example, the electron density plot for $Ga_{16}N_{15}O$ corresponds to the state at the Γ point at −1.8 eV in Fig. 2.

For the $1\times1\times1$ cell, the states near the Fermi surface (Fig. 4) show strong hybridization and admixture of O 2*s*-, O 2*p*-, Ga 4*s*-, Ga 4*p*-, N 2*s*-, and 2*p*-like states, indicating their delocalized nature. The so-called donor level indeed forms a band extending throughout the space. In the $2\times2\times2$ supercell, the PDOS from distant Ga and N atoms has significantly decreased. The contribution from the O 2*s*-like state appears to gain in strength compared to that of the O 2*p*-like states, and the same is true from the nearest Ga atom. The mixing between the Ga 4*s*-like state and that of O 2*s*-like state appears to be comparable. The electron density plot in Fig. 5 for the Γ point state shows the starting localization of the donor electrons. For the $3\times3\times2$ supercell, the contribution from distant oxygen and gallium atoms is even less pronounced, and there is a stronger mixing of states from the oxygen impurity and neighboring gallium atoms. This localization process can be seen more clearly for the case of the $4\times4\times3$ unit cell in Fig. 5. There is an increasing mixing of the Ga 4*s*-like and O 2*s*-like states compared to the 2*p*-like states of both atoms. The corresponding electronic density plot shows a strong *s*-like distribution near the oxygen impurity and very little delocalization even at the nearest Ga atom. This seems surprising considering the significant contribution from Ga 4*s*-like states. However, the 4*s*-like states have increasing density closer to the center of the bond than to the nucleus, and thus increasing density near the oxygen atom indicates that although the electron spends more time in an orbital composed of Ga 4*s*-like states, the nature of hybridization locates it closer to oxygen atoms or nitrogen atoms than the Ga atom itself. This is clear in Fig. 5.

The distribution of electron density near the Fermi surface clearly shows that localization monotonically progresses with increasing supercell size or decreasing oxygen contribution. This localization effect was further explored in the *xy* plane with $2\times2\times1$, $4\times4\times1$, and $6\times6\times1$ supercells. The corresponding plots of electron density are shown in Fig. 6. The electron distribution is shown for the lowest conduction state, as in Fig. 5. It appears that at a higher dilution, for example, ppt or ppm concentration, the electron in the donor state would be more localized near the oxygen site. The donor could be described as O_N^X, with the excess electron occupying a state composed of O 3*s*- and Ga 4*s*- and 4*p*-like character yielding an *s*-like distribution around the defect site. In this sense, this is similar to the electronic distribution of a F center associated with anion vacancies. For example, in an ionic crystal such as potassium chloride, a vacancy at the chlorine site would appear positive to the rest of the lattice and thus would capture an electron. This electron

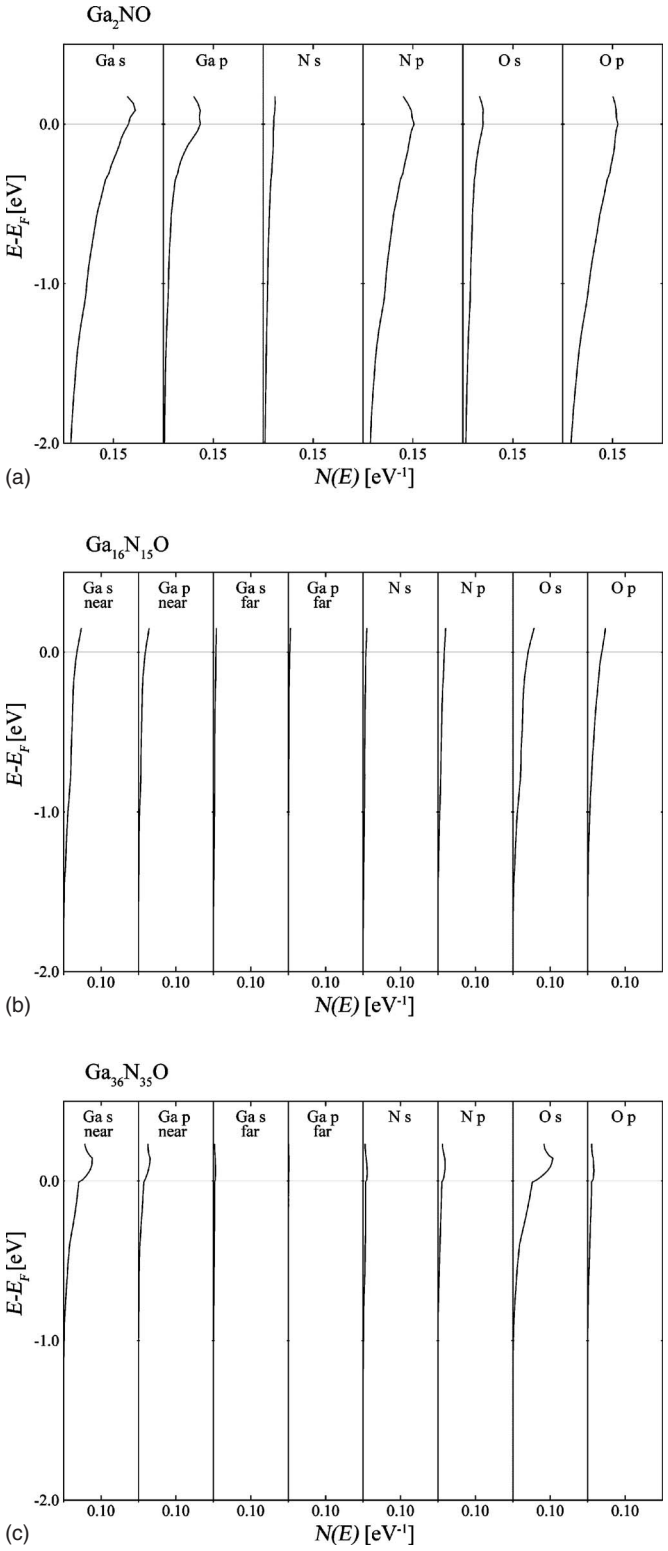

FIG. 4. Partial DOS (PDOS) of the lowest conduction band for Ga_2NO (a), $Ga_{16}N_{15}O$ (b), and $Ga_{36}N_{35}O$ (c). The figures show the PDOS of O, one of the nearest gallium atoms Ga, and a pair of Ga and N atoms far removed. For this metallic compounds, E_F is chosen as the top of the occupied donor states. The Fermi energy E_F is the zero of the energy scale.

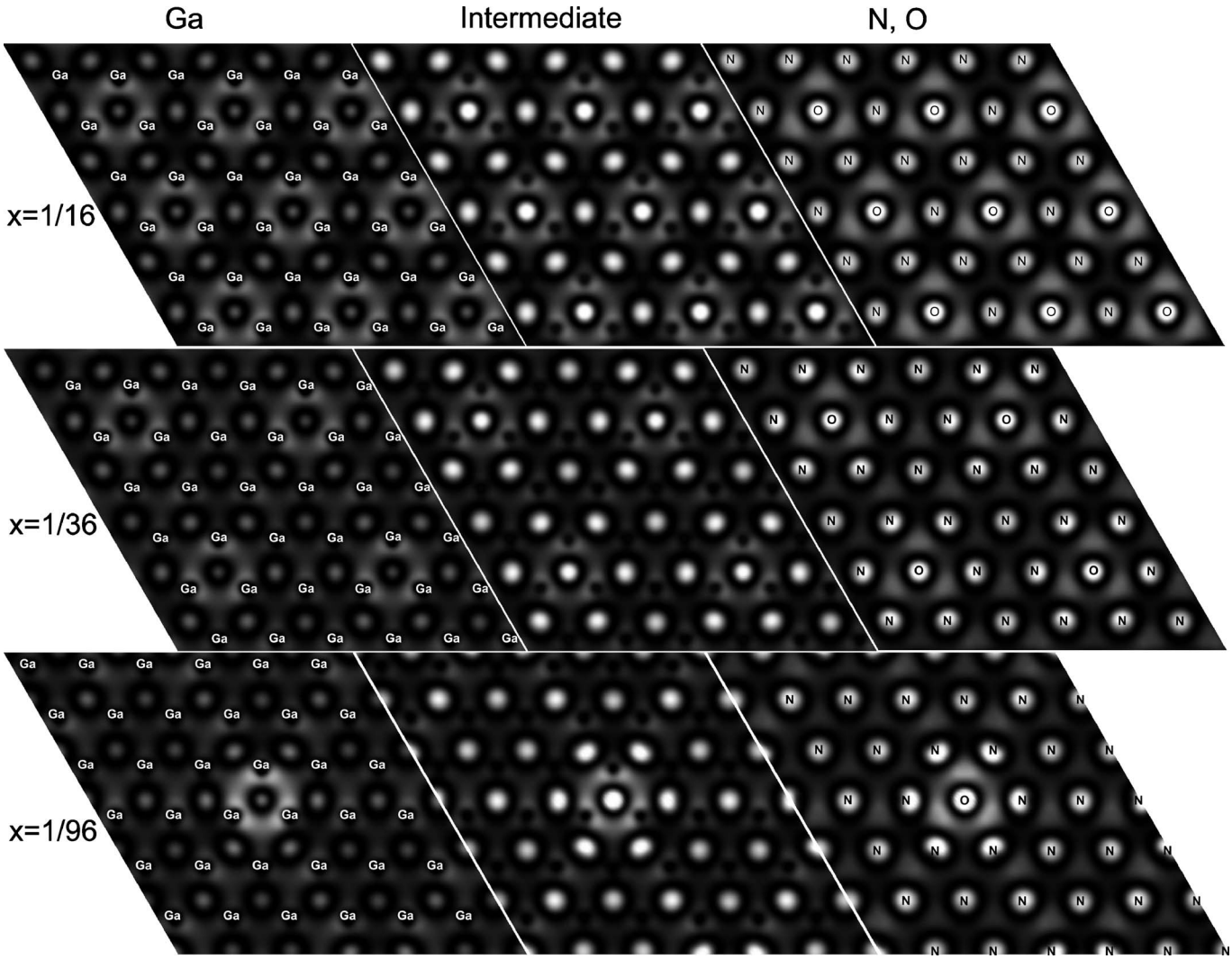

FIG. 5. Electron density distribution for the lowest conduction (donor) state in the vicinity of the oxygen impurity (for $Ga_{16}N_{15}O$, the state at the Γ point is at −1.8 eV, see Fig. 2). The density is shown for three *xy* planes, the planes containing O and neighboring Ga, and the plane intermediate between these two planes. The plots correspond to the oxygen concentration $GaN_{1-x}O_x$, $x=1/6$, $1/36$, and $1/96$.

would be localized near the F center, the corresponding molecular orbital being composed of K 4*s*-like states. Similarly, an O^{-2} ion at N^{3-}, i.e., $O_N^{\bullet}$, would appear positively charged with respect to the rest of the lattice and could become a neutral O_N^X center with the capture of an electron. However, the corresponding state is a state from the bottom of the conduction band composed of Ga- and O-antibonding states, with the corresponding electron localized around the oxygen atom. Unlike the F center, the associated donor energy level is a shallow impurity level lying within a few meV below the bottom of the conduction band, as observed in optical measurements.[11] The critical density indicating a transition from a delocalized to an extended state could not be determined since the process of localization appears to be a monotonic process.

C. Variation of the formation energy of GaN:O with oxygen concentration

Finally, we have studied the change of the formation energy $\Delta E_{f,n}$ by the process of gradually substituting N by O. Within the same supercell ($Ga_{36}N_{36-n}O_n$) crystal structure, we have calculated the formation energy for the reaction,

$$Ga_iN_{i-n}O_n + \frac{1}{2}O_2 \rightarrow Ga_iN_{i-n-1}O_{n+1} + \frac{1}{2}N_2; \Delta E_{f,n},$$

with $i=36$ and $n=0-3$. The calculation has been performed using the VASP code in the GGA with an energy cutoff of 520 eV and using the tetrahedron method to calculate the total energy. To incorporate the local relaxation of the atoms around the defect, we have optimized the structure, taking fixed lattice constants of the pure GaN compound.

The change of the total energy $\Delta E_{f,n}$ as a function of the O concentration is displayed in Fig. 7. We have found for the unit cell considered here that isolated O_N defects are energetically favored compared to associate O_N defects. Therefore, in Fig. 7, we have given the energy values only for isolated defects. One sees in Fig. 7 that the change in the formation energy decreases with increasing *n*. However, because of the size of the unit cell, we could not increase the

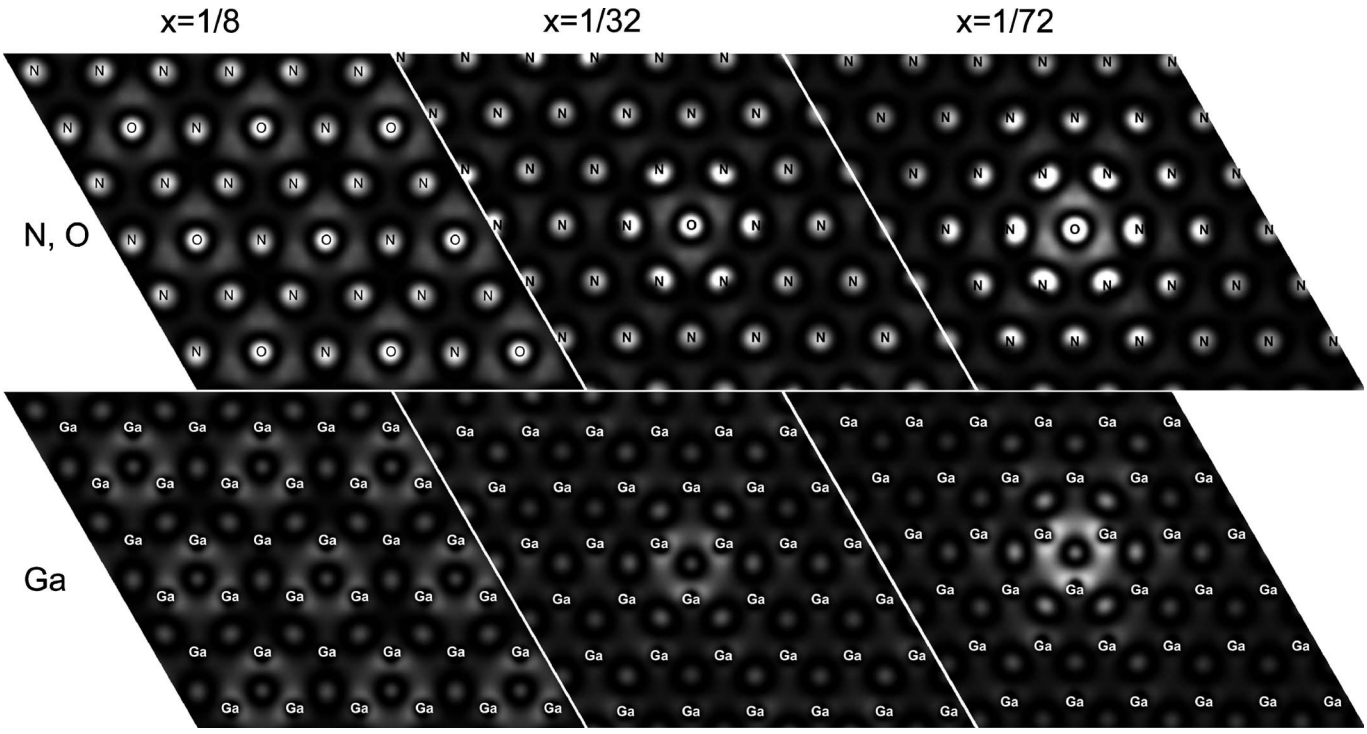

FIG. 6. Electron density distribution for the lowest conduction (donor) state in the vicinity of the oxygen impurity (for $Ga_{16}N_{15}O$, the state at the Γ point is at −1.8 eV, see Fig. 2). The density is shown for the planes containing O and neighboring Ga. The plots correspond to lattices where one N is substituted by an O in the cells $(2a,2b,1c)$, $(4a,4b,1c)$, and $(6a,6b,1c)$ with $a=b=3.216$ Å and $c=5.234$ Å. This results in oxygen concentrations $GaN_{1-x}O_x$, $x=1/8$, $1/32$, and $1/72$, respectively.

number of O atoms any further, as for $n>3$ it is not possible anymore to construct a defect structure of only isolated O substitution defects.

IV. DISCUSSION

The main objective of this computational investigation is to understand the nature of local geometry and donor states associated with oxygen impurities at nitrogen sites in GaN. Oxygen atoms easily replace nitrogen atoms in GaN. Concentration levels can reach almost 25 at. % without affecting its wurtzite structure. Thus, the $O_N^{X,\bullet}$ centers in GaN provide an excellent opportunity to theoretically investigate its electronic structure and local structural modifications using supercells of varying dimensions.

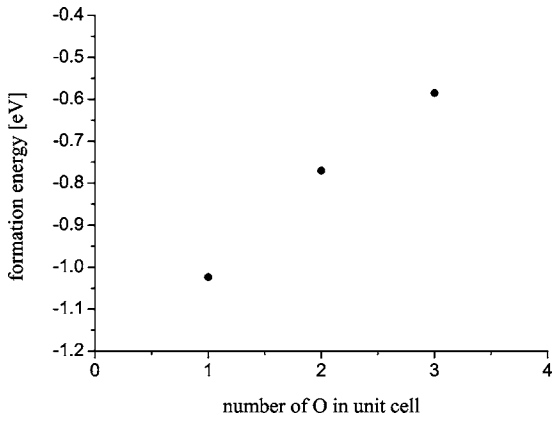

FIG. 7. Formation energy for the reaction $Ga_iN_{i-n}O_n+\frac{1}{2}O_2 \rightarrow Ga_iN_{i-n-1}O_{n+1}+\frac{1}{2}N_2$; $\Delta E_{f,n}$, with $i=36$ and $n=0-3$.

Oxygen atoms at nitrogen sites do not significantly affect the local geometries. The observed Ga-O bond lengths in GaN from the EXAFS measurements[10] are in good qualitative agreement with those calculated from theory although the tendency for shorter bond lengths experimentally observed is not reproduced in the theoretically optimized geometries. This discrepancy is not due to the *n*-type behavior of the materials, as shown from the calculations involving exact charge compensation using Zn-O substitutional couples.

The manner in which the band parameters such as the Fermi level and energy gap change with oxygen concentration has been shown. However, the most interesting results from this study concern the nature of localization of the donor state. At the level of dilution investigated in this study, the charge distribution of the electron from the donor impurity O_N^X indicates an extended state. With increasing dilution, this state appears to be spatially localized near the impurity ion with a predominantly *s*-like character similar to F centers in alkaline halides. It appears that this localization monotonically increases with decreasing impurity concentration.

Conventionally, the role of impurity ions in semiconductors is discussed using rigid band models describing the energy bands of the host materials and appropriate donor or acceptor levels for the impurity ions located within the forbidden gap. This is a realistic description of the electronic structure of a doped semiconductor in situations for deep

levels at low dopant concentrations (10^{17}–10^{20} cm^{-3}) and dopants with incomplete *f* or *d* shells. In the latter case, the dopant electron resides in a localized atomiclike state. Even at very high concentrations, the corresponding donor levels, particularly for rare earth ion impurities, are highly localized and the corresponding energy bands do not show dispersion in the *k* space similar to the bands originating from the core electron levels. However, this is not the case for an O_N^X center.

A neutral oxygen atom at the N site has to accommodate three electrons donated by a Ga atom. This oxygen atom acquires a closed shell configuration, $2s^2 2p^6$, using two of the three electrons. The third electron has to occupy an otherwise unoccupied state from the bottom of the conduction band unless a divalent ion substitutes for a trivalent gallium ion. The corresponding donor orbital is thus expected to be a linear combination of atomic orbitals associated with the nearest neighbors, Ga. More accurately, it is an antibonding state formed from O- and Ga-like states. Since this orbital is obtained due to the lowering of a state from the conduction band, the corresponding energy level will lie close in energy to the bottom of the conduction band, and the associated wave function will have a significant overlap with other extended states at the bottom of the conduction band. From the first order perturbation theory, it can be easily shown that the first order correction to the wave function will lead to a significant mixture of the donor wave function with the extended states near the bottom of the conduction band. Thus, with increasing oxygen concentration, these perturbed wave functions will overlap through the admixture of the extended states of the host and will start forming an energy band. Unlike the deep level or the localized impurity states, the states associated with O_N^X will rapidly lead to delocalized states with increasing oxygen concentration. This is essentially reflected in the results discussed earlier with supercells ranging from typical unit cells to $3\times3\times2$ supercells.

Optically, these impurity bands will shift the band gap to a lower value. Even with modest oxygen concentrations, GaN:O will behave like a material with a smaller optical gap, rather than a host lattice with discrete impurity states.

ACKNOWLEDGMENT

This work was partially supported by U.S. Department of Energy under Contract No. DE-FC26-04NT42274.

[1] Solid State Lighting Program Planning Report, Prepared by Navigant Consulting, Inc. for U.S. Department of Energy (February 3–4, 2005, San Diego) (available at www.netl.doe.gov/ssl).

[2] H. Wu, J. Hunting, F. J. Di Salvo, and M. G. Spencer, Phys. Status Solidi C **2**, 2074 (2005); H. Wu, C. B. Poitras, M. Lipson, M. G. Spencer, J. Hunting, and F. J. Di Salvo, Appl. Phys. Lett. **88**, 011921 (2006).

[3] R. Garcia, G. A. Hirata, M. H. Farias, and J. McKittrick, Mater. Sci. Eng., B **90**, 7 (2002); S. Faulhaber, L. Loeffler, J. Hu, E. Kroke, and R. Riedel, J. Mater. Res. **18**, 2350 (2003).

[4] N. H. Tran, R. N. Lamb, L. J. Lai, and Y. W. Yang, J. Phys. Chem. B **109**, 18348 (2004).

[5] *CRC Handbook of Chemistry and Physics*, 83rd ed. (CRC, Boca Raton, FL, 2002).

[6] K. S. A. Butcher, H. Timmers, Afifuddin, P. P.-T. Chen, T. D. M. Weijers, E. M. Goldys, T. L. Tansley, R. G. Elliman, and J. A. Freitas, Jr., J. Appl. Phys. **92**, 3397 (2002).

[7] M. Marezio and J. P. Remeika, J. Chem. Phys. **46**, 1862 (1967).

[8] J. Ahman, G. Svensson, and J. Albertson, Acta Crystallogr., Sect. C: Cryst. Struct. Commun. **52**, 1336 (1996); S. Geller, J. Chem. Phys. **33**, 676 (1960).

[9] P. Kroll, R. Dronskowski, and M. Martin, J. Mater. Chem. **15**, 3296 (2005).

[10] M. J. Ariza, A. Koo, H. J. Trodahl, B. J. Ruck, A. Bittar, D. J. Jones, B. Bonet, J. Kozière, and J. Moscovici, Surf. Interface Anal. **37**, 273 (2005).

[11] M. A. Reschikov and H. Morkoc, J. Appl. Phys. **97**, 061301 (2005).

[12] F. A. Kroger, *The Chemistry of Imperfect Crystals* (North-Holland, New York, 1962).

[13] G. Kresse and J. Hafner, Phys. Rev. B **48**, 13115 (1993); **49**, 14251 (1994); G. Kresse and J. Furthmueller, Comput. Mater. Sci. **6**, 15 (1996); Phys. Rev. B **54**, 11169 (1996).

[14] A. R. Williams, J. Kübler, and C. D. Gelatt, Phys. Rev. B **19**, 6094 (1979).

[15] P. E. Blöchl, Phys. Rev. B **50**, 17953 (1994).

[16] G. Kresse and D. Joubert, Phys. Rev. B **59**, 1758 (1999).

[17] J. P. Perdew, J. A. Chevary, S. H. Vosko, K. A. Jackson, M. R. Pederson, D. J. Singh, and C. Fiolhais, Phys. Rev. B **46**, 6671 (1992).

[18] V. Eyert, Hahn-Meitner-Institute Report No. B548, 1997 (unpublished).

[19] U. v. Barth and L. Hedin, J. Phys. C **5**, 1629 (1972).

[20] X.-L. Chen, J.-K. Liang, Y. P. Xu, P. Z. Jiang, Y.-D. Yu, and K. Q. Lu, Mod. Phys. Lett. B **13**, 285 (1999).

[21] M. Suzuki, T. Uenoyama, and A. Yanase, Phys. Rev. B **52**, 8132 (1995).

[22] W. H. Strehlow and E. L. Cook, J. Phys. Chem. Ref. Data **2**, 163 (1973).

[23] R. W. Godby, M. Schlüter, and L. J. Sham, Phys. Rev. B **36**, 6497 (1987).